ARTICLES

Novel Gemini Micelles from Dimeric Surfactants with Oxyethylene Spacer Chain. Small Angle Neutron Scattering and Fluorescence Studies

Soma De,[†] Vinod K. Aswal,[‡] Prem S. Goyal,[‡] and Santanu Bhattacharya*[,†]

Department of Organic Chemistry, Indian Institute of Science, Bangalore 560 012, India, and Solid State Physics Division, Bhabha Atomic Research Centre, Bombay 400 085, India

Received: January 22, 1998; In Final Form: May 4, 1998

Three new gemini surfactants containing mono-, di-, and trioxyethylene spacer chains have been synthesized. Small angle neutron scattering (SANS) cross sections from the micellar aggregates of these dimeric amphiphiles Br^-, n-$C_{16}H_{33}NMe_2^+-CH_2(CH_2OCH_2)_pCH_2-N^+Me_2$-$n$-$C_{16}H_{33}$, Br^-, (where $p = 1$, 2, and 3) in aqueous media (D_2O) have been measured. The data have been analyzed using the Hayter and Penfold model for macro-ion solution to compute the interparticle structure factor $S(Q)$ taking into account the screened Coulomb interactions between the dimeric micelles. The SANS analysis showed that the micellar morphology depends on both the nature and the length of the spacer unit. Detailed analysis of the data further indicates that the introduction of oxyethylene spacer is not sufficient enough to prevent looping of the spacer chain. Thus the average separation between the dimethylammonium ion headgroups is considerably lower than is expected from a fully extended conformation of the spacer chain. The micelles from these surfactants have also been characterized in terms of their critical micelle concentrations (cmc), microviscosities, and micropolarities on the basis of the information provided by micelle-solubilized fluorescent probes. These results indicate little difference in their micellar properties such as cmc, microviscosity, and micropolarity.

Introduction

Dimeric or *gemini* surfactants, consisting of two hydrophobic chains and two polar headgroups covalently attached through a spacer, e.g., **1** (16-*m*-16, $2Br^-$) are of current interest[1] owing to their unusual properties, such as low critical micellar concentrations (cmc), high viscoelasticities, and enhanced abilities for lowering the oil−water interfacial tension.[2] Recently, it has been shown that aqueous dispersions of dimeric surfactants, 16-*m*-16, $2Br^-$ with *m*-value ≤ 4, have high propensity for micellar growth[3] and generally produce threadlike micelles. In contrast, the ones with $m \geq 5$ generate either ellipsoidal or spherical micelles. Since the polar headgroups are *connected* within a gemini surfactant by a covalent linkage, the separation between the polar headgroups within a dimeric unit depends on both the nature (rigid vs flexible) and the length of the spacer chain.

$$n\text{-}C_{16}H_{33}N^+Me_2(CH_2)_mN^+Me_2n\text{-}C_{16}H_{33}$$
$$2Br^- \qquad\qquad 2Br^-$$

1

Attempts to correlate the aggregate properties with that of the molecular features of surfactant are important for developing new surfactant systems for specific applications. Owing to our continuing interest in the understanding of the aggregation behavior from amphiphilic molecules of varying architectures,[4] we developed a range of new surfactant systems. Various physical methods are currently available to examine the nature of aggregation. Among these, the neutron scattering technique offers ample opportunity to study the aggregate organizations formed from different surfactants.[5−8] This is especially useful with micellar solutions of dimeric surfactants where the effect of spacer chain looping can be conveniently examined by this noninvasive technique. On the basis of the above reasoning, we already examined the small angle neutron scattering (SANS) spectra of the micelles formed from dimeric surfactants, 16-*m*-16, $2Br^-$, **1**, where, $m = 3$, 4, 5, 6, 8, 10, and 12, and their mixed systems with CTAB.[9,10] These studies clearly indicate that the extent of aggregate growth, and the variations of shapes of the dimeric micelles and mixed micelles depend primarily on the spacer chain length (*m*-value) in **1**.

In aqueous solution, the two covalently connected positively charged $-NMe_2^+$ headgroups within a 16-*m*-16, $2Br^-$ unit tend to maintain a critical distance between them to minimize the Coulombic repulsion. But since such situation creates rather an unfavorable contact of the hydrophobic $(CH_2)_m$ spacer chain with the bulk water, a separation based on the compromise of these two opposing tendencies results. One can therefore anticipate that a replacement of CH_2 by oxygen in selected positions of the spacer chain would affect its looping in a different fashion as compared to the dimeric surfactants that contain polymethylene spacer. As a consequence, this might enhance the tendency of the spacer chain containing oxyethylene

* To whom the correspondence should be addressed. Fax: 91-080-334-1683. E-mail: sb@orgchem.iisc.ernet.in. Also at the Chemical Biology Unit, Jawaharlal Nehru Centre for Advanced Scientific Research, Jakkur, Bangalore 560 064, India.
[†] Indian Institute of Science.
[‡] Bhabha Atomic Research Centre.

S1089-5647(98)00836-0 CCC: $15.00
Published on Web 07/17/1998

to fold in association with water molecules present at the stern layer region. In other words, additional hydration at the level of spacer chain should mitigate the Coulombic repulsion between the two cationic $-NMe_2^+$ centers. However, dimeric biscationic surfactants with spacer containing oxyethylene groups are hitherto not developed. Only recently, Rosen et al. has reported a group of dimeric, *anionic* surfactants with two carboxylate groups prepared from diepoxy compounds.[11] In this paper, we introduce new dimeric surfactants with three different oxyethylene spacers, i.e., *n*-$C_{16}H_{33}N^+Me_2(CH_2)(CH_2OCH_2)_p$-$(CH_2)N^+Me_2$*n*-$C_{16}H_{33}$, $2Br^-$, **2**, where $p = 1, 2, 3$, and the results of our SANS studies on these dimeric cationic surfactants. The hydrocarbon chain length in these surfactants is equal to that present in the corresponding monomeric, cationic surfactant, cetyltrimethylammonium bromide (CTAB). To understand the role of "wettable" spacer chain in determining the morphologies of dimeric surfactant micelles, we have performed SANS experiments employing the above gemini micelles. The variation of concentration and the effect of temperature on the neutron cross sections were also looked upon. We have also examined the mixed micelles of known compositions of CTAB and various dimeric surfactants, 16-$CH_2-(CH_2OCH_2)_p-CH_2$-16, $2Br^-$, **2**. Finally, to rationalize the information obtained from SANS studies with other micellar properties, we have measured their critical micellar concentrations, microviscosities, and micropolarities.

$$n\text{-}C_{16}H_{33}N^+Me_2CH_2(CH_2OCH_2)_pCH_2N^+Me_2n\text{-}C_{16}H_{33}$$
$$2Br^- \qquad\qquad 2Br^-$$
2a-2c, $p = 1, 2, 3$.

Experimental Section

Materials. All the reagents and solvents were highest grade available commercially and used purified, dried, or freshly distilled as required. Cetyltrimethylammonium bromide (CTAB), *n*-hexadecyl bromide, phosphorus tribromide, diethylene glycol, triethylene glycol, tetraethylene glycol, and pyrene were purchased from Aldrich Chemical Co. *N*,*n*-Hexadecyl-*N*,*N*-dimethylamine was obtained by refluxing *n*-hexadecyl bromide with dimethylamine (Merck, 40% aqueous solution) in dry ethanol at 80 °C for 24 h. The dimeric surfactants 16-*m*-16, $2Br^-$, **1**, were prepared as described.[9a] Steam-distilled water was used for all physical measurements.

Dimeric Surfactants. The dimeric surfactants, **2**, were synthesized as indicated in the following (Scheme 1).

SCHEME 1[a]

$$HOCH_2(CH_2OCH_2)_pCH_2OH \xrightarrow{a} \textbf{3a-3c}, p = 1,2,3$$

$$BrCH_2(CH_2OCH_2)_pCH_2Br \xrightarrow{b} \textbf{4a-4c}, p = 1, 2, 3$$

$$n\text{-}C_{16}H_{33}N^+Me_2CH_2(CH_2OCH_2)_pCH_2N^+Me_2n\text{-}C_{16}H_{33}$$
$$2Br^- \qquad\qquad 2Br^-$$
2a-2c, $p = 1, 2, 3$

[a] (a) PBr_3, ~80−90% yield; (b) $C_{16}H_{33}NMe_2$ (3.0 equiv), dry EtOH, reflux, 72−96 h, 70−90% yield.

Synthesis of Dibromides (4a−4c). The dibromo precursors (**4a**−**4c**) were synthesized by the addition of PBr_3 to the individual diol in a dropwise manner over a period of 1 h at 0 °C. Then the mixtures were stirred with concomitant heating at 50−60 °C for 12 h. The reaction mixture was then cooled to ambient temperature and dissolved in $CHCl_3$ (25 mL). Water was added slowly, and the mixture was transferred into a separatory funnel. The organic layer was separated out after washing with water, $NaHCO_3$, and again with water and finally passed through a bed of anhydrous Na_2SO_4. The resulting $CHCl_3$ solution was concentrated and loaded on a silica gel column (60−120 mesh) and was eluted with hexane to give a colorless liquid (yield 80−90%). All the dibromides gave satisfactory ^1H NMR spectra.

*Bis(2-bromoethyl) Ether (**4a**).* ^1H NMR (200 MHz, $CDCl_3$) δ 3.48 (t, 4H), 3.84 (t, 4H).

*1,2-Bis(2-bromoethoxy)ethane (**4b**).* ^1H NMR (200 MHz, $CDCl_3$) δ 3.48 (t, 4H), 3.69 (s, 4H), 3.84 (t, 4H).

*Bis(5-bromoethoxyethyl) Ether (**4c**).* ^1H NMR (200 MHz, $CDCl_3$) δ 3.45 (t, 4H), 3.65 (s, 8H), 3.81 (t, 4H).

Synthesis of Bis(quaternary ammonium) Surfactants (2a−2c). The bis(quaternary ammonium) surfactants **2a**−**2c** were synthesized as described in the following.

All the surfactants **2a**−**2c** were obtained by refluxing the corresponding α,*w*-dibromoalkoxyalkanes with *N*,*n*-hexadecyl-*N*,*N*-dimethylamine in dry ethanol at ~80 °C for 72−96 h. At the end of this period, solvent was removed under vacuum from the reaction mixture, and the solid thus obtained was recrystallized several times from 10 mL of acetone containing 2 drops of methanol to obtain solid surfactants as pure product as determined from ^1H NMR spectra and elemental analysis. The overall yields of the surfactants ranged from 50 to 60%.

*Bis(hexadecyl dimethylammonium)diethyl Ether (**2a**).* Mp 230 °C (softening), 245−250 °C; ^1H NMR (200 MHz, $CDCl_3$) δ 0.88 (t, 6H, alkyl chain 2 × 1 C*H*$_3$), 1.18−1.32 (s + br m, 52H, alkyl chain 2 × 13 C*H*$_2$), 1.58−1.72 (br m, 4H, alkyl chain 2 × 1 C*H*$_2$CH$_2$N$^+$), 3.42 (s, 12H, 2 × 2 N$^+$C*H*$_3$), 3.54 (crude t, 4H, alkyl chain 2 × 1 C*H*$_2$N$^+$), 3.99 (br s, 4H, spacer chain 2 × 1 C*H*$_2$N$^+$), 4.31 (br s, 4H, spacer chain 2 × 1 OC*H*$_2$CH$_2$N$^+$). C, H, N analysis, Calcd for $C_{40}H_{86}N_2OBr_2$, 0.5 H_2O: C 61.62, H 10.99, N 3.59. Found: C 61.33, H 11.24, N 3.48.

*Bis(hexadecyl dimethylammonium)diethoxyethane (**2b**).* Mp 200 °C (softening), 215−220 °C; ^1H NMR (200 MHz, $CDCl_3$) δ 0.88 (t, 6H, alkyl chain 2 × 1 C*H*$_3$), 1.25−1.34 (s + br m, 52H, alkyl chain 2 × 13 C*H*$_2$), 1.65−1.74 (br s, 4H, alkyl chain 2 × 1 C*H*$_2$CH$_2$N$^+$), 3.44 (s, 12H, 2 × 2 N$^+$C*H*$_3$), 3.50−3.63 (m, 4H, alkyl chain 2 × 1 C*H*$_2$N$^+$), 3.97 (br s, 4H, spacer chain 2 × 1 C*H*$_2$N$^+$), 4.16 (br s, 4H, spacer chain 1 × 1 OC*H*$_2$C*H*$_2$O), 4.33 (br s, 4H, spacer chain 2 × 1 OC*H*$_2$CH$_2$N$^+$). C,H,N analysis, Calcd for $C_{42}H_{90}N_2O_2Br_2$, 1.0 H_2O: C 60.56, H 11.13, N 3.36. Found: C 60.51, H 11.27, N 3.03.

*Bis(hexadecyl dimethylammonium)bis(ethoxyethyl) Ether (**2c**).* Mp 205 °C (softening), 235−240 °C; ^1H NMR (200 MHz, $CDCl_3$) δ 0.88 (t, 6H, alkyl chain 2 × 1 C*H*$_3$), 1.25−1.34 (s + br m, 52H, alkyl chain 2 × 13 C*H*$_2$), 1.72 (br s, 4H, alkyl chain 2 × 1 C*H*$_2$CH$_2$N$^+$), 3.44 (s, 12H, 2 × 2 N$^+$C*H*$_3$), 3.54−3.63 (crude t, 8H, alkyl chain 2 × 1 C*H*$_2$N$^+$ and spacer chain 1 × 2 C*H*$_2$N$^+$), 3.99 (br s, 8H, spacer chain 1 × 4 OC*H*$_2$C*H*$_2$O), 4.33 (br s, 4H, spacer chain 1 × 2 OC*H*$_2$CH$_2$N$^+$). C,H,N analysis, Calcd for $C_{44}H_{94}N_2O_3Br_2$: C 61.52, H 11.03, N 3.26. Found: C 61.62, H 11.33, N 3.13.

Methods. Descriptions of analytical and spectroscopic instruments have been published previously.[9a]

Fluorescence Measurements. Steady-state fluorescence measurements were performed in a Hitachi F-4500 fluorescence

spectrophotometer equipped with a thermostated water-circulating bath (Julabo model F10). All the measurements were carried out at 30 °C and using a 3 cm^3 cell. Pyrene, a fluorescence probe the spectral signature of which changes with the formation of the micelle, was chosen as a probe for the cmc (critical micellar concentration) determinations. Excitation wavelength was fixed at 337 nm, and the emission spectra for the range 360−410 nm was examined. Bandwidths were fixed at 5 nm for both the emission and the excitation. Surfactant solutions of different compositions in water were doped with pyrene. The cmc values were determined from the plots of the concentration of the surfactant vs the ratio (I_1/I_3) of the intensities of the first (I_1) and the third (I_3) vibronic peaks in the fluorescence emission spectra due to pyrene solubilized in respective micellar aggregates.[12] The micropolarities of the surfactant micelles were characterized by the value of I_1/I_3.

Determination of Microviscosities ($\bar{\eta}$). The fluorescence anisotropies (r) of 1,6-diphenyl-1,3,5-hexatriene (DPH), as sensed by DPH doped in micelles, were measured from the intensities obtained at 0−0°, 0−90°, 90−0°, and 90−90° angle settings of the excitation and emission polarization accessories, respectively. The temperature of the cuvette containing the sample was maintained at 30 °C with the aid of a thermostated temperature controlling water-circulating bath (Julabo model F10). The fluorescence intensities of the emitted light polarized parallel ($I_{||}$) and perpendicular ($I_{\perp}$) to the exciting light were recorded and were corrected for the scattered light intensity, which was determined independently for an unlabeled reference suspension by the same procedure. The fluorescence anisotropy (r) for each micellar sample at 30 °C was calculated according to $r = (I_{||} - G\cdot I_{\perp})/(I_{||} + 2\cdot G\cdot I_{\perp})$, where G is the grating correction factor. Microviscosities ($\bar{\eta}$) of the individual micellar systems in which the fluorophore was placed were calculated from the anisotropy values.[13] The measurements were done at a fixed 50 mM concentration for **2a**−**2c** and at 100 mM concentration of CTAB.

Determination of the Compositions of the Mixed Micelles. The composition of the mixed micelles was calculated according to Clint's theory, as described previously,[10] which assumes an ideal mixing of the surfactant components.

Small Angle Neutron Scattering (SANS) Measurements. Small angle neutron scattering (SANS) is a well-established technique to investigate the structural aspects of materials on a length scale of 10−1000 Å.[14] As reported earlier,[5−7] these measurements provide useful information pertaining to the shapes of various self-organizing systems in a noninvasive manner. Recently, we examined the role of spacer chain length (m) on the morphology of dimeric micelles using the SANS experiments.[9] To explore whether the incorporation of "O" in place of some $-CH_2-$'s within spacer chain has any role in dictating the micellar morphology, we have now carried out similar studies of the dimeric surfactant system 16-$CH_2-(CH_2OCH_2)_p-CH_2$-16, $2Br^-$, where $p = 1, 2, 3$. We have also compared various micellar parameters from these newly developed surfactants with the corresponding dimeric surfactant (16-m-16, $2Br^-$, **1**) devoid of any oxygen atom in the spacer.

All the final solutions used in the neutron-scattering experiments were prepared in D_2O (at least 99.5 atom % D pure). This provides a good contrast between the micelle and the solvent in a SANS experiment. Neutron-scattering measurements were performed on the 7.0 m (source-to-detector distance) SANS instrument at the CIRUS Reactor, Trombay.[15] In this setup, the sample-to-detector distance is 1.8 m for all the runs. This spectrometer uses a BeO filtered beam and has a resolution ($\Delta Q/Q$) of about 15% at $Q = 0.05$ $Å^{-1}$. The angular distribution of the scattered neutrons is recorded using a one-dimensional position-sensitive detector. The accessible wave vector transfer, Q ($=4\pi \sin {}^1/_2\phi/\lambda$, where λ is the wavelength of the incident neutrons and ϕ is the scattering angle), range of this instrument is between 0.02 and 0.3 $Å^{-1}$. The wavelength is $\lambda = 0.52$ nm. The SANS data from the above instrument are normalized to absolute scale by comparing the data against those from Porasil A11.[16]

The solutions were held in a 0.5 cm path-length UV grade quartz sample holder with tight-fitting Teflon stoppers, sealed with Parafilm. In most of the measurements, the surfactant concentration ($c = 50$ mM) and the sample temperature (30 ± 0.1 °C) were kept fixed. The effect of different concentration on the SANS distribution was also studied for 16-$CH_2-(CH_2OCH_2)_2-CH_2$-16, $2Br^-$, **2b**, micellar sample for concentration in the range of 30−70 mM at 40 °C. The effect of temperature was also investigated for this surfactant system at a fixed surfactant concentration of $c = 50$ mM. In the mixed micellization studies, where each of the above gemini surfactants was separately mixed with CTAB, the percentages of dimeric surfactants in the micelles of binary surfactant mixtures were 23.1 mol %.

Data Treatment. Scattering intensities from the surfactant solutions were corrected for detector background, empty cell scattering, and sample transmission. The resulting corrected intensities were normalized to absolute cross-section units, and thus $d\Sigma/d\Omega$ vs Q was obtained. This absolute calibration has an estimated uncertainty of 10%. In figures, the Q-axis has been plotted in log scale to indicate the peak position clearly. The experimental points are fitted using a nonlinear least-squares routine as described below. Comparisons between the experimental and the calculated cross sections are shown in Figures 1−4.

SANS Analysis

1. Calculation of the Scattering Intensity. The coherent differential scattering cross-section, ($d\Sigma/d\Omega$), derived by Hayter and Penfold[17] and Chen,[14] can be reduced to eq 1 for an assembly of *monodisperse*, uniform ellipsoidal micelles

$$d\Sigma/d\Omega = n(\rho_m - \rho_s)^2 V_m^2[\langle F^2(Q)\rangle + \langle F(Q)\rangle^2\{S(Q) - 1\}] + B \quad (1)$$

where n denotes the number density of the micelles, ρ_m and ρ_s are, respectively, the scattering length densities of the micelle and the solvent, and V_m is the volume of the micelle. $F(Q)$ is the single particle form factor, and $S(Q)$ is the interparticle structure factor. B is a constant term that represents the incoherent background. For the analysis, we assume the micelles to be monodisperse prolate ellipsoids, ($a = c \neq b$), where a sphere is a special case of that. The aggregation number N for the micelle is related to the micellar volume V_m by the relation $N = V_m/v$, where v is the volume of the individual surfactant molecule. Then the eq 1 can be rewritten as

$$d\Sigma/d\Omega = 1/N(c - c_m)V_m^2(\rho_m - \rho_s)^2[\langle F^2(Q)\rangle + \langle F(Q)\rangle^2\{S(Q) - 1\}] + B \quad (2)$$

where $(c - c_m) = nN$, c_m is the cmc, and c is the surfactant concentration.

The volume of the mixed micelle was calculated as described in our previous paper[10] by eq 3

$$V_m = N(x_1 v_{CTAB} + (1 - x_1)v_{16-CH_2-p-CH_2-16}) = (N_{CTAB}v_{CTAB} + N_{16-CH_2-p-CH_2-16}v_{16-CH_2-p-CH_2-16}) \quad (3)$$

where v_{CTAB} and $v_{16-CH_2-p-CH_2-16}$ are the volumes of CTAB and gemini surfactant, respectively. $N=(N_{CTAB}+N_{16-CH_2-p-CH_2-16})$, N_{CTAB}, and $N_{16-CH_2-p-CH_2-16}$ are the aggregation numbers of CTAB and gemini surfactant in the mixed micelle, respectively.

The scattering length density of mixed micelle is obtained from eq 4

$$\rho_m = (x_1\rho_{CTAB} + (1 - x_1)\rho_{16-CH_2-p-CH_2-16}) \quad (4)$$

where ρ_{CTAB} and $\rho_{16-CH_2-p-CH_2-16}$ are the scattering length densities due to CTAB and 16-CH_2-*p*-CH_2-16, $2Br^-$ surfactants, respectively, and x_1 is the mole fraction of CTAB in the mixed micelle.

For an ellipsoidal particle

$$\langle F^2(Q)\rangle = \int_0^1 [F(Q,\mu)]^2 \, d\mu \quad (5)$$

and

$$\langle F^2(Q)\rangle^2 = [\int_0^1 F(Q,\mu)\, d\mu]^2 \quad (6)$$

where μ is the cosine of the angle between the axis of resolution and Q.

The form factor, $F(Q, \mu)$ is given by the eq 7, i.e.

$$F(Q,\mu) = 3(\sin w - w\cos w)/w^3 \quad (7)$$

where $w = Q[a^2\mu^2 + b^2(1-\mu^2)]^{1/2}$ and a and b are, respectively, the semiminor and semimajor axes of the ellipsoid of revolution.

2. Structure Factor for Interacting Micelles. The interparticle structure factor $S(Q)$ depends on the spatial distribution of micelles. In the following analysis, we have calculated $S(Q)$ using mean spherical approximation as developed by Hayter and Penfold.[17b] This theory is applicable if there is no angular correlation between the particles. This assumption is quite reasonable for *charged* micelles especially when the surfactant concentration is low and the ratio of the axes is not much greater than unity. Strong electrostatic repulsions prohibit close proximity between two micelles. It may be mentioned that satisfactory data analysis procedures for ellipsoidal particles have not been developed. Though the approximation of treating ellipsoid as a sphere has been often used in the literature,[14] its consequences on size parameters are not fully understood. The intermicellar interaction is modeled via a screened Coulomb potential, and $S(Q)$ is calculated in mean spherical approximation. On the basis of such consideration in the following, the ellipsoidal micelle is approximated by an equivalent sphere of radius $R = (a^2b)^{1/3}$. In this analysis, the only unknown parameters in $d\Sigma/d\Omega$ are the effective monomer charge, α, and the aggregation number, N. The ellipsoidal micelles, in general, could have polydispersity in their sizes. However, we have assumed them to be monodisperse for the simplicity of the calculation and limit the number of unknown parameters in the analysis.

Here, it should be worthwhile to mention that the analysis assuming core + shell model of micelle would probably be more accurate. However, this will also increase the number of unknown parameters in the fitting, such as thickness of the shell, number of "wet" methylene units, etc. Therefore, for simplicity, we assumed the present model, which was also used in the previous reports.[9b]

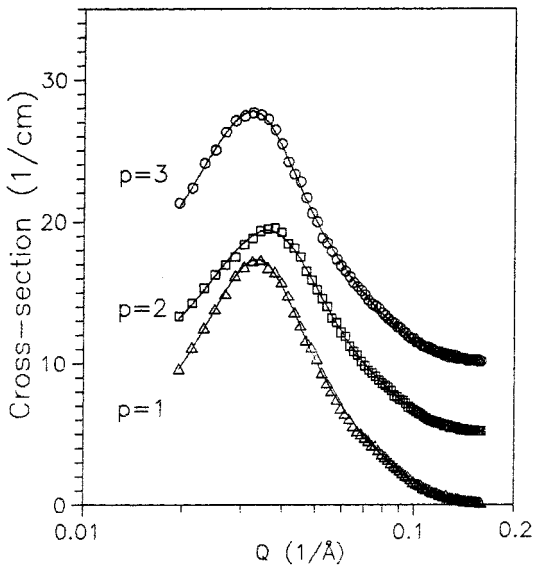

Figure 1. SANS distributions from dimeric micellar systems **2a**−**2c** at specified concentration (50 mM) at 30 °C. The lines shown are theoretical fits, and the solid marks are experimentally determined data points. The SANS distributions for $p = 2$ and 3 are shifted vertically by 5 and 10 units, respectively.

The data in Figure 1 (corresponding to different $p = 1$, 2, and 3) were first analyzed in terms of eq 2. N, a, and α were taken as the parameters of the fit, and v was calculated using Tanford's formula: $v = (1052 + 53.8 + 73 \times p)$ Å^3, where 1052 Å^3 is the volume of two tails with the headgroups, 53.8 Å^3 is the volume of two $-(CH_2)-$ units, and 73 Å^3 is the volume of a ethylene oxide ($-CH_2-O-CH_2-$) group.[18] The contribution of scattering from bound counterions is very small because of small volume of counterions and relatively poor contrast. Hence the volume of the counterion Br^- is not considered for their contributions to the scattering. The solid lines in Figure 1 are the calculated curves. The major axis b ($3Nv/4\pi a^2$) was obtained from a knowledge of the above parameters. The values of N, α, a, b, and v are given in Table 1. The axial ratios of **2a**−**2c** are also compared with that of 16-*m*-16, $2Br^-$ in Table 1. The effects of concentration and temperature on size parameters for **2b** are shown in Figures 2 and 3. The data in Figure 4 corresponds to mixed micelles composed of 100 mM CTAB with 30 mM **2b** and 16-6-16, $2Br^-$ respectively.

Results and Discussion

Molecular Features and Solubilities of New Geminis. From the earlier studies,[9] we found that the length and the nature of the spacer chain connecting the two headgroups mainly determine the micellar morphology in the case of the dimeric surfactants (16-*m*-16, $2Br^-$). SANS studies further indicated that the dimeric surfactants, 16-*m*-16, $2Br^-$ form disk or cylindrical micelles for $m \leq 4$ and ellipsoidal or spherical micelles for $m \geq 5$. With the replacement of some $-CH_2-$'s in the spacer chain with $-O-$, one would anticipate some changes in the conformation of the latter. In addition the presence of $-O-$ in the spacer chain will make the same relatively more hydrophilic. Another point of worth consideration is that the C−O−C bond angle (115.8°) is higher than the C−C−C (112.2°) bond angle when the spacer chain remains in an extended *s*-trans conformation. This would render the

TABLE 1: Effect of Spacer Chain in Micellar Systems, 2a−2c, on *Q* Value.[a] The *b*/*a* Values of 16-*m*-16, 2Br$^-$ (m = 5, 8, and 10)[b] Are Given for Comparison

entry no.	surfactant	aggregtion no. N	effective monomer charge α	monomer vol. v (Å^3)	semiminor axis $a = c$ (Å)	semimajor axis b (Å)	b/a
1	**2a**	220	0.062	1179	25.6	94.3	3.68
2	16-*5*-16	238	0.11	1187	24.2	115.0	4.75
3	**2b**	165	0.066	1252	24.8	80.2	3.23
4	16-*8*-16	72	0.29	1267	22.8	42.0	1.82
5	**2c**	226	0.058	1325	25.8	107.6	4.17
6	16-*10*-16	83	0.2	1321	22.6	45.2	1.95

[a] All the SANS spectra were taken at 30 °C using 50 mM 16-CH_2−(CH_2OCH_2)$_p$−CH_2-16, 2Br$^-$ and 16-*m*-16, 2Br$^-$ micelles. [b] Taken from ref 9b.

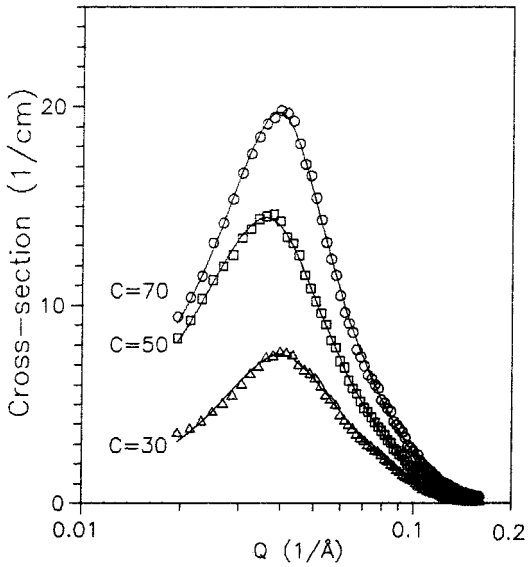

Figure 2. SANS distributions from dimeric micelles **2b** at different concentrations: 30 mM (△), 50 mM (□), and 70 mM (○) at 40 °C.

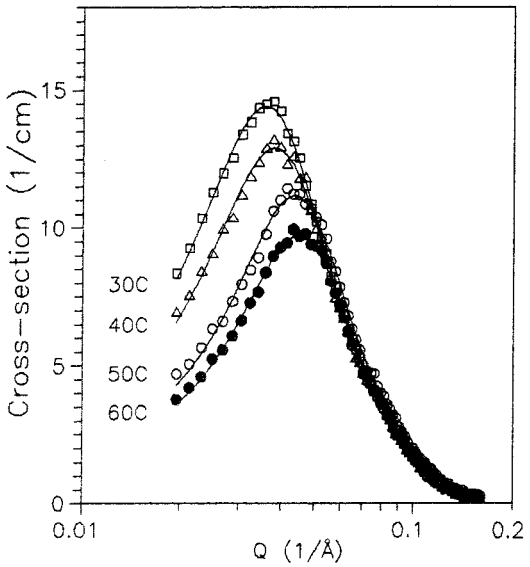

Figure 3. SANS distributions from dimeric micelles **2b** at various temperatures: 30 °C (□), 40 °C (△), 50 °C (○), and 60 °C (●).

chain little more flexible. Keeping these aspects in mind, we have synthesized three new gemini surfactants having variable number of oxygens in the spacer chain.

All the new surfactants **2a**−**2c** could be readily dissolved in D_2O and remained optically translucent for several weeks. The SANS analysis showed that, at a fixed concentration (50 mM) of the dimeric surfactants, the micellar structures of **2a**−**2c** are different. Since the spacer chain lengths of **2a**−**2c** are

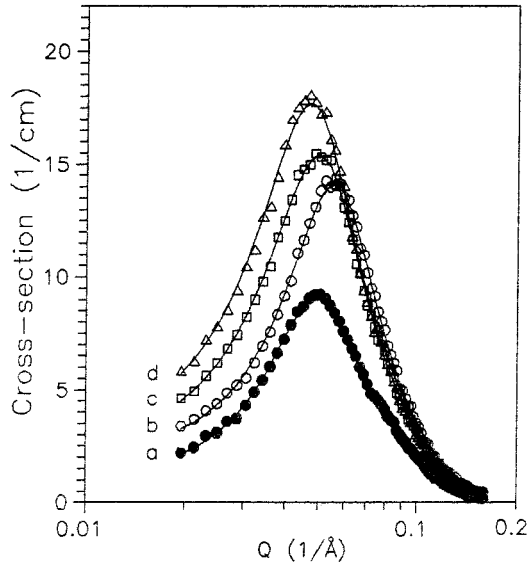

Figure 4. SANS distributions from pure CTAB and the mixed micelles of 30 mM **2b** and 16-*6*-16, 2Br$^-$ dimeric systems with 100 mM CTAB: (a) 100 mM CTAB (●), (b) 160 mM CTAB (○), (c) 100 mM CTAB + 30 mM 16-*6*-16, 2Br$^-$ (□), and 100 mM CTAB + 30 mM **2b** (△) at 30 °C. The lines shown are theoretical fits, and the solid marks are experimentally determined data points.

comparable with that of 16-*5*-16, 2Br$^-$, 16-*8*-16, 2Br$^-$, and 16-*10*-16, 2Br$^-$, respectively, as obtained from the molecular modeling studies (INSIGHT II 2.3.5 package, Biosym. Technologies), most of the time we have compared their micellar properties against those of 16-*m*-16, 2Br$^-$, m = 5, 8, 10.

Neutron Cross Sections. We first describe the results of the measurements of neutron cross sections from the micellar solutions of dimeric surfactants 16-CH_2−(CH_2OCH_2)$_p$−CH_2-16, 2Br$^-$ in D_2O as a function of p values at a fixed surfactant concentration (50 mM) and temperature (30 °C). Measurements have covered Q ranges from 0.02 to 0.16 Å^{-1}. SANS distributions for 50 mM 16-CH_2−(CH_2OCH_2)$_p$−CH_2-16, 2Br$^-$, p = 1, 2, and 3, show well-defined peaks characteristic of dispersions of charged particles as is the case with pure 50 mM 16-*m*-16, 2Br$^-$ solution. This peak arises because of a corresponding peak in the interparticle structure factor $S(Q)$. Usually, this peak occurs at $Q_m \sim 2\pi/d$, where d is the average distance between the micelles. Since the Q_m was found to differ with p, one can easily conclude that the number density (n) of micelles is not the same in above samples even when they have identical surfactant concentration. The above observations further imply that the aggregation number of the micelle, N, depends on the length and the nature of the spacer unit. It is, however, not apparent from this that the micelles are spherical. Consequently, in the following analysis, we assume them to be prolate ellipsoids, ($a = c \neq b$), sphere being a special case of that.

TABLE 2: Average Separation[a] between the Two Me_2N^+ Headgroups within Dimeric Micelles 2a−2c and Comparison with That Obtained from Molecular Modeling within a Gemini.[b] Corresponding Values for 16-*m*-16, $2Br^-$ (*m* = 5, 8, and 10)[c] Are Given for Comparison

entry no.	surfactant	avg. separation between headgroups in micelles (Å)	calcd distance between the two Me_2N^+ headgroups within a gemini (Å)
1	**2a**	9.45	7.64
2	16-*5*-16	11.1	7.82
3	**2b**	10.12	11.33
4	16-*8*-16	14.4	11.72
5	**2c**	9.79	14.2
6	16-*10*-16	13.6	14.27

[a] Obtained assuming it to be equal to $\sqrt{(4\pi a_{\text{eff.}}{}^2/N)}$, where $a_{\text{eff.}} = (a^2b)^{1/3}$, considering the micelles to be *ellipsoidal* as found from SANS data. [b] Calculated using INSIGHT II 2.3.5 package, Biosym. Technologies assuming the spacer chain is in a fully extended conformation. [c] Taken from ref 9a.

For **2a**, which has one oxygen in the spacer, the micelles are less ellipsoidal compared to 16-*5*-16, $2Br^-$ micelles[9] (Table 1). For **2b**, the aggregation number, *N*, decreases compared to that for **2a** but again increases for **2c**. But, the effective fractional charge (α) does not differ much. The axial ratio (*b*/*a*) is less for **2b** compared to **2a** but more with respect to the corresponding surfactant without oxygen 16-*8*-16, $2Br^-$; i.e., the micelle size increases. Similar comparison for **2c** shows that the micelles of **2c** are more ellipsoidal compared to either **2a** or **2b**. Though the lengths of the spacer chain in **2c** and 16-*10*-16, $2Br^-$ are comparable in their extended conformations, the micelles of **2c** are more ellipsoidal than that of the gemini surfactant, 16-*10*-16, $2Br^-$, in which the spacer chain is devoid of oxygen. Therefore, one can anticipate a dissimilar spacer chain conformation in **2c** as compared to 16-*10*-16, $2Br^-$ owing to large differences in the axial ratios. It seems that the changes are connected with the increase in the length and the flexibility of the spacer as well as its accessibility to water.

SANS data (Table 2) show that the incorporation of −O− in place of a $-CH_2-$ decreases the distance between the headgroups of the gemini surfactant compared to that in 16-*m*-16, $2Br^-$. If the spacer chain looping alone governs the micellar structure, then an increase in the spacer chain length (and hence looping) from **2a** to **2b** should make the micelles of **2b** more spherical than the micelles of **2a**. Since the micelles of **2b** are found to be more spherical than those of **2a**, the spacer chain in **2b** is not significantly more hydrophilic than that in **2a.** Thus even after incorporation of an additional O in **2b**, the spacer in **2b** prefers to loop deeper into the micellar interior. However, in **2c**, the hydration of the spacer appears to be significant. In such situation the cationic headgroups should come considerably closer although the mutual electrostatic repulsion is probably compensated by the additional hydration at the trioxyethylene spacer chain. Thus, owing to combination of looping and hydration of the spacers in **2a**−**2c**, the situation appears to be more complex (see below).

Packing Parameter. As stated earlier, the insertion of a spacer unit between two $-NMe_2^+$ ions at the level of headgroups imposes additional geometric constraints on the surfactant intramolecular packing. This is reflected in the aggregate morphology. The packing parameter (*P*), introduced by Israelachvili et al.,[19] is related to aggregate morphology in aqueous solutions at a concentration higher than the critical micellar concentration (cmc) by the equation $P = v/l \cdot A$, where v is the effective volume occupied by the hydrophobic moiety of the surfactant molecule, l is the critical length in the fully extended conformation, and A is the surface area occupied by a surfactant headgroup at the water/micelle hydrophobic core interface. Both l and v can be calculated using Tanford's equations.[20] As long as the hydrophobic tail length is constant, l is likely to remain the same throughout all the surfactants **2a**−**2c** and v should increase marginally (relative %) with the change in the length of the spacer since the length of the two hydrophobic tails has been kept unchanged. The effective headgroup area A is decided by the effective charge on the headgroup and by the size of the headgroup. Therefore, this is an important quantity for the dimeric surfactants, which is mainly responsible for the change in the packing parameter. It is clear from Table 1 that the effective headgroup charge (α) is almost the same for all the three new dimeric surfactant systems in the corresponding micellar aggregates. Therefore, the change in A or packing parameter is expected to be largely due to the alterations in the conformation of the spacer, which is found to follow a *non*monotonic dependence. For the dimeric surfactant with short spacer, i.e. **2a**, because of the Coulombic repulsion between the headgroups, the spacers are stretched to adopt more extended conformation. The length of the spacer to be stretched is decided by the charge on the headgroup. In particular, with 16-*m*-16, $2Br^-$ systems, we found that A approaches a maximum surface area occupied by its surfactant headgroups at the water/micelle hydrophobic core interface for $m = 8$. Here, for $p = 1$, i.e., with the incorporation of one oxygen in the spacer, the length of the spacer chain becomes lesser than that in 16-*5*-16, $2Br^-$, thus increasing the Coulombic repulsion between the headgroups. Then the micelles of **2a** should be more elliptical than those of 16-*5*-16, $2Br^-$. But the stabilizing interaction between the spacer chain and water somewhat neutralizes the repulsion and gives rise to less ellipsoidal morphology for **2a** compared to 16-*5*-16, $2Br^-$. For $p = 2$, the length of the spacer is now longer than the critical distance necessary to minimize Coulombic repulsion between $-NMe_2^+$ groups to maintain the equilibrium distance. So it can now loop as the Coulombic repulsion has not increased since the charge on the headgroup remains the same. It can be understood that owing to the increase in A, the packing parameter decreases; hence, the micelles become less ellipsoidal. For $p = 3$, A decreases owing to a folded arrangement of the spacer, thereby increasing the packing parameter. So, it forms more elliptical micelles. It is possible that under this situation, the spacer chain is also more hydrated making the micelles of **2c** more "wet".

Separation between the Two Polar Headgroups within a Dimeric Surfactant. In aqueous solution, the two covalently connected positively charged $-NMe_2^+$ headgroups within a dimeric surfactant unit tend to maintain a critical distance between them to minimize the electrostatic repulsion. But since such situation creates a rather undesirable contact of the spacer chain with the bulk water especially when the spacer chain is hydrophobic, a separation based on the compromise of these two opposing tendencies results. In **2a**−**2c**, spacers are relatively more hydrophilic than 16-*m*-16, $2Br^-$. We have estimated this critical distance on the basis of the SANS data, assuming it to be equal to $\sqrt{(4\pi a_{\text{eff.}}2/N)}$, where $a_{\text{eff.}} = (a^2b)^{1/3}$, considering the micelles to be *ellipsoidal*. Applying this, we obtained a value of $a_{\text{eff.}} \sim 7.94$ Å for CTAB ($m = 0$), which is in reasonable agreement with the value reported by Zana et al.[2] In the same way, we obtained the critical distances between the two cationic centers for **2a**−**2c**, which came out to be 9.45, 10.12, and 9.79 Å respectively (Table 2). Examination of the data suggests that the average separation between the cationic headgroups in these micelles is smaller than that for the

TABLE 3: Effects of Change in Surfactant (2b) Concentrations on *Q* Value at 40 °C

entry no.	concn (mM)	aggregation no. *N*	effective monomer charge α	monomer vol. *v* (Å^3)	semiminor axis $a = c$ (Å)	semimajor axis *b* (Å)	*b*/*a*
1	30	100	0.12	1252	24.8	48.7	1.96
2	50	145	0.075	1252	24.8	70.3	2.83
3	70	179	0.07	1252	24.8	87.1	3.51

TABLE 4: Effect of Temperature on *Q* Value for the Micellar 2b at a Fixed 50 mM Concentration

temp. (°C)	aggregation no. *N*	effective monomer charge α	monomer vol. (Å^3)	semiminor axis *a* (Å)	semimajor axis *b* (Å)	*b*/*a*
30	165	0.066	1252	24.8	80.2	3.23
40	145	0.075	1252	24.8	70.3	2.83
50	109	0.011	1252	24.8	52.8	2.13
60	101	0.116	1252	24.8	49.1	1.98

corresponding dimeric surfactant system, **1**, containing $(CH_2)_m$ spacers, which proves that indeed the stabilizing interaction between the spacer and water partly overcomes the Coulombic repulsion, thus decreasing the critical distance between the two cationic centers.

Effect of Surfactant Concentration Variation. The effect of surfactant concentration on SANS distributions is shown in Figure 2 for **2b** at 40 °C. As already indicated, the peak in $d\Sigma/d\Omega$ occurs at $Q_m = 2\pi/d$, where *d* is the average distance between the micellar particles. With an increase in concentration, the interparticle distance decreases and the peak shifts to lower *Q* values. The concentration range examined was from 30 to 70 mM. It is seen that the calculated distributions give the peak positions in $d\Sigma/d\Omega$ with a good correspondence with experimentally determined points. As the concentration of **2b** is decreased, it is found that the peak in the measured distribution broadens with significant shifts in the peak position. The micellar shape changes from $b/a \sim 1.96$ to $b/a \sim 3.51$ upon increase in concentration of **2b** from 30 to 70 mM (Table 3) owing to the formation of more prolate ellipsoidal micellar shape at higher concentration. Increasing *N* for a given spacer chain length results in an increase in the axial ratio (*b*/*a*); i.e., as *N* increases, micellar shape tends to become more prolate ellipsoidal. Since the shape of the micelle changes with respect to concentration, the interactions among charged headgroups of the dimeric **2b** units and water in the Stern layer region of the micelle appear to play an important role in determining the micellar shape. The effective fractional charge on the dimeric units of **2b** decreases with increase in concentration.

Effect of Temperature. Previously, we have carried out the SANS experiments to show how micellar size varies with temperature for polymethylene spacer containing gemini micelles and their mixed systems with single-chain surfactant. Figure 3 shows the variation of neutron cross sections for **2b** micelles as the temperature is increased. The neutron cross sections build up at higher *Q* values as the temperature is increased. The peak in the measured distribution also broadens with the increase in temperature.

Table 4 records the information based on the above experimental findings as a function of temperature. Increase in temperature enhances the degree of ionization and thus effects a modification of the magnitude of electrostatic repulsion. This results in a decrease in the aggregation number, *N*, upon the increase in temperature. The effective fractional charge per monomer, however, appears to increase with increase in temperature. Since a smaller effective charge indicates a more ellipsoidal morphology, increasing temperature appears to induce ellipsoid-to-sphere transition. This notion is also supported by the concomitant decrease in *b*/*a* values upon increase in temperature.

TABLE 5: Dependence of the Critical Micellar Concentrations, Microviscosities,[a] and Micropolarities of 16-CH_2−$(CH_2OCH_2)_p$−CH_2-16, 2Br$^-$ Dimeric Micelles as a Function of *p*-Value at 30 °C

entry no.	surfactant	cmc × 10^5 (M)	microviscosity ($^-\eta$)[a] (P)	I_1/I_3
1	**2a**	1.9 ± 0.15	1.116	1.028
2	**2b**	1.7 ± 0.15	1.205	1.029
3	**2c**	2.0 ± 0.15	1.146	1.024

[a] Measured at 50 mM concentration for 16-CH_2−$(CH_2OCH_2)_p$−CH_2-16, 2Br$^-$ dimeric micelles at 30 °C.

Critical Micellar Concentrations. The critical micellar concentration (cmc) data for 16-CH_2-$(CH_2OCH_2)_p$-CH_2-16, 2Br$^-$ series have been summarized in Table 5. The respective plots of the concentrations of the new surfactant solutions vs the ratios (I_1/I_3) of the intensities of the first (I_1) and the third (I_3) vibronic peaks in the fluorescence emission spectra due to solubilized pyrene gave apparent breaks related to critical micellar concentrations (not shown). In contrast to the dimeric surfactant containing polymethylene spacer, which showed a sharp break, these presently described surfactants **2a**−**2c** showed rather broad breaks in the above plots. This may be due to the tendency of these micelles to form premicellar aggregates prior to formation of gemini micellar aggregates. Evidence of premicellar aggregation was also reported by Zana et al.[21a] for gemini amphiphilic 8-*3*-8, 2Br$^-$ and 8-*6*-8, 2Br$^-$ systems during the determination of their cmc by the electrical conductivity method. Another point to note is that there is little difference in the cmc values among **2a** to **2c**. It is possible that the probe pyrene used in this experiment may not be sensing the differences in the relative wetnesses of the micelles.

Dependence of Microviscosity ($\bar{\eta}$). Another parameter of considerable interest is the microenvironmental viscosity (microviscosity, $\bar{\eta}$) of the dimeric micellar aggregates. This parameter can be conveniently estimated by the determination of the fluorescence polarization of the probe, 1,6-diphenyl-1,3,5-hexatriene (DPH).[13] Table 5 summarizes the microviscosity estimates of 16-CH_2−$(CH_2OCH_2)_p$−CH_2-16, 2Br$^-$ micelles at a fixed concentration of 50 mM as a function of variable *p* values. DPH is a fluorescence probe whose emission quantum yield gets enhanced upon partitioning into a micelle or a bilayer from water. The microviscosity we have measured agrees for CTAB (100 mM) with that reported using DPH and other probes, around 0.56 P for CTAB.[22] We have observed that the microviscosities of 16-*m*-16, 2Br$^-$ systems decreased with the increase in *m* values. But, there is not much difference in the microviscosities of **2a**−**2c**. Though the microviscosity of **2a** is very close to that of 16-*5*-16, 2Br$^-$, the microviscosities of **2b** and **2c**, despite having longer spacer length, are very different from that of 16-*m*-16, 2Br$^-$, $m \geq 8$. They are closer to that of 16-*5*-16, 2Br$^-$.

Dependence of Micropolarity (I_1/I_3). Table 5 also lists the values of the pyrene intensity ratio for the surfactant micelles investigated at 30 °C. The measurements were performed at

TABLE 6: Values of Various Parameters for the Mixed Micelles of Pure CTAB and 30 mM 16-*6*-16, 2Br$^-$ and 2b with 100 mM CTAB Obtained from Fits to the Experimental Data

concn (mM)	aggregation no.[a] N	effective monomer charge α	monomer vol. v (Å^3)	semiminor axis $a = c$ (Å)	semimajor axis b (Å)	b/a
100 mM CTAB	160	0.10	560	22.0	44.5	2.02
160 mM CTAB	168	0.09	560	22.0	46.5	2.11
23.1 mol % 16-*6*-16 in CTAB	175	0.082	560 (CTAB) 1213 (16-*6*-16)	22.0	61.1	2.78
23.1 mol % **2b** in CTAB	200	0.07	560 (CTAB) 1252 (**2b**)	22.0	71.2	3.24

[a] N is the equivalent aggregation number of monomers.

surfactant concentrations 2 wt %, where the probe is fully partitioned in the micelles. These values suggest that though the micellar shapes are different for **2a**−**2c** owing to different surfactant packing parameter, there is very little effect on the micropolarity sensed by pyrene. Since, the value of I_1/I_3 depends on the chemical composition of the medium surrounding the probe, it prompted us to believe that the local composition at the micelle solubilization site of pyrene is virtually the same irrespective of the nature of the spacer unit. Since pyrene solubilizes preferentially in the palisade layer of the cationic micelles, the variations of I_1/I_3 with the spacer unit simply reflect the changes of composition of the palisade layer. However, notably in general, the I_1/I_3 values of **2a**−**2c** are slightly higher than that of the 16-*m*-16, 2Br$^-$ system presumably owing to presence of oxygen atom in the spacer, although we do not see any significant rise in the I_1/I_3 value of **2b** and **2c**.

Mixed Micellization Studies with CTAB. Since the surfactant mixtures bear potential for numerous applications and also play a pertinent role in other solubilization processes,[23] we considered that it may be worthwhile to examine the mixed micellization behavior of the presently developed new gemini surfactants with the commonly used monomeric surfactant, CTAB. Toward this direction, we already reported the SANS studies of different mixed micelles composed of dimeric surfactant, 16-*m*-16, 2Br$^-$ (where *m* is devoid of any oxygen atom) and CTAB.[10] This allowed the long ellipsoidal micelle due to 16-*m*-16, 2Br$^-$ to undergo a transition to a more spherelike micelle in the resulting mixed micelles.

The SANS measurements for the mixed micellar solutions of **2b** and 16-*6*-16, 2Br$^-$ with 100 mM CTAB were carried out at 23.1 mol % of dimeric surfactants at 30 °C in D_2O. For comparison, the data for a pure 100 and 160 mM CTAB solutions are also shown (Figure 4, Table 6). As the experimental cmc values for the mixed micellar solution matched well with the theoretical values, we assumed that the dimeric surfactants **2b** and 16-*6*-16, 2Br$^-$ mixed ideally with CTAB. With the same percentage of dimeric surfactants in the mixed micelles, the position of maximum intensity (Q_m) shifts to a lower Q value with a concomitant increase in the maximum intensity for **2b** compared to 16-*6*-16, 2Br$^-$. This is reflected in the equivalent aggregation number of monomers, the axial ratio (b/a) of the micelle, and the effective fractional charge (α) on micelles. This suggests that a lesser number of $-CH_2-$ groups in the spacer chain protrude into the shell when **2b** is incorporated into the mixed micelle. Thus the mixed micelles of **2b**/CTAB are more ellipsoidal in nature than that of 16-*6*-16, 2Br$^-$/CTAB.

Conclusions

Dimeric surfactants (16-$CH_2-(CH_2OCH_2)_p-CH_2$-16, 2Br$^-$ system) in which two quaternary ammonium centers are attached at the level of polar headgroup by a mono-, di-, or trioxyethylene spacer chain ($p = 1$, 2, and 3) have been synthesized. For these dimeric surfactant micelles, the SANS spectra were measured and the cmc values were determined using an extrinsic fluorescence probe, pyrene. From the measurements of small-angle neutron-scattering cross sections, it is shown that the micellar structures of the 16-$CH_2-(CH_2OCH_2)_p-CH_2$-16, 2Br$^-$ system change with p values. The micellar morphology was found to depend on both the nature and the length of the spacer chain. The fractional charge is less and the minor axis is high for these new dimeric micelles compared to that of the 16-*m*-16, 2Br$^-$ system, which contained only polymethylene spacer. The presence of three oxygen atoms in the spacer chain of **2c** appears to make the spacer chain loop as the distance between the cationic dimethylammonium ion centers is shorter in this case than that in **2b**. It is therefore possible that micelles of **2c** are possibly more wet owing to additional ability of the spacer chain in **2c** to assocaite with interfacially located water molecules. This additional hydration shields should assist in bringing the $-NMe_2^+$ headgroups closer despite unfavorable electrostatic consequences. Although fluorescence studies do not show much dependence of critical micellar concentrations or micropolarities on the spacer unit, it may be possible that the microenvironments around the probe molecules may not be sensing the finer aspects of hydration and looping especially if the probes are located deeper inside the micellar interior.

Acknowledgment. We thank the Inter University Consortium for financial support of this work. We also thank Dr. B. A. Dasannacharya for his encouragement and interest in this work.

References and Notes

(1) Rosen, M. J. *Chemtech* **1993**, *23*, 30.
(2) Zana, R.; Talmon, Y. *Nature* **1993**, *362*, 228.
(3) Karaborni, S.; Esselink, K.; Hilbers, P. A. J.; Smit, B.; Karthauser, J.; van Os N. M.; Zana, R. *Science* **1994**, *266*, 254.
(4) (a) Bhattacharya, S.; De, S. *J. Chem. Soc., Chem. Commun.* **1995**, 651. (b) Bhattacharya, S.; De, S. *J. Chem. Soc., Chem. Commun.* **1996**, 1283. (c) Bhattacharya, S.; De, S.; George, S. K. *J. Chem. Soc., Chem. Commun.* **1997**, 2287. (d) Bhattacharya, S.; Haldar, S. *Langmuir* **1995**, *11*, 4748. (e) Bhattacharya, S.; Snehalatha, K. *Langmuir* **1995**, *11*, 4653. (f) Bhattacharya, S.; Haldar, S. *Biochim. Biophys. Acta (Biomembranes)* **1996**, *1283*, 21. (g) Bhattacharya, S.; Subramanian, M.; Hiremath, U. *Chem. Phys. Lipids* **1995**, *78*, 177. (h) Bhattacharya, S.; Subramanian, M. *J. Chem. Soc., Perkin Trans. 2* **1996**, 2027. (i) Bhattacharya, S.; Snehalatha, K. *J. Chem. Soc., Perkin Trans. 2* **1996**, 2021. (j) Subramanian, M.; Mandal, S. K.; Bhattacharya, S. *Langmuir* **1997**, *13*, 153. (k) Bhattacharya, S.; Snehalatha, K. *Langmuir* **1997**, *13*, 378. (l) Bhattacharya, S.; Snehalatha, K. *J. Org. Chem.* **1997**, *62*, 2198. (m) Bhattacharya, S.; Snehalatha, K.; George, S. K. *J. Org. Chem.* **1998**, *63*, 28.
(5) (a) Berr, S. S.; Jones, R. R. M.; Johnson, J. S. *J. Phys. Chem.* **1992**, *96*, 5611. (b) Berr, S. S.; Jones, R. R. M. *Langmuir* **1988**, *4*, 1247.
(6) (a) Pilsl, H.; Hoffmann, H.; Hoffmann, S.; Kalus, J.; Kencono, A. W.; Lindner, P.; Ulbricht, W. *J. Phys. Chem.* **1993**, *97*, 2745. (b) Chevalier, Y.; Zemb, T. *Rep. Prog. Phys.* **1990**, *53*, 279. (c) Kaler, E. W.; Billman, J. F.; Fulton, J. L.; Smith, R. D. *J. Phys. Chem.* **1991**, *95*, 458. (d) Prasad, D.; Singh, H. N.; Goyal, P. S.; Rao, K. S. *J. Colloid Interface Sci.* **1993**, *155*, 415. (e) Goyal, P. S.; Menon, S. V. G.; Dasannacharya, B. A.; Thiyagarajan, P. *Phys. Rev.* **1995**, *51E*, 2308.

(7) Goyal, P. S.; Dasannacharya, B. A.; Kelkar, V. K.; Manohar, C.; Rao, K. S.; Valaulikar, B. S. *Physica B* **1991**, *174*, 196.

(8) Hirata, H.; Hattori, N.; Ishida, M.; Okabayashi, H.; Frusaka, M.; Zana, R. *J. Phys. Chem.* **1995**, *99*, 17778.

(9) (a) De, S.; Aswal, V. K.; Goyal, P. S.; Bhattacharya, S. *J. Phys. Chem.* **1996**, *100*, 11664. (b) Aswal, V. K.; De, S.; Goyal, P. S.; Bhattacharya, S.; Heenan, R. K. *Phys. Rev.* **1998**, *57E*, 776.

(10) De, S.; Aswal, V. K.; Goyal, P. S.; Bhattacharya, S. *J. Phys. Chem. B* **1997**, *101*, 5639.

(11) Zhu, Y.; Masuyama, A.; Kobata, Y.; Nakatsuji, Y.; Okahara, M.; Rosen, M. J. *J. Colloid Interface Sci.* **1993**, *158*, 40.

(12) Kalyanasundaram, K. *Photochemistry in Microheterogeneous Systems*; Academic Press: New York, 1987; p 177.

(13) Shinitzky, M.; Barenholz, Y. *Biochim. Biophys. Acta* **1978**, *515*, 367.

(14) (a) Chen, S. H. *Annu. Rev. Phys. Chem.* **1986**, *37*, 351. (b) Chen, S. H.; Lin, T. L. *Methods of Experimental Physics*; Academic Press: New York, 1987; Vol. 23B, p 489.

(15) Goyal, P. S.; Aswal, V. K.; Joshi, J. V. BARC Report, I/018, 1995; Bhabha Atomic Research Centre: Bombay, India, 1995.

(16) (a) Wignal, G. D.; Bater, F. S. *J. Appl. Crystallogr.* **1987**, *20*, 40. (b) Dr. G. D. Wignal of the Oak Ridge National Laboratory, Oak Ridge, TN, has kindly supplied us with this standard sample.

(17) (a) Hayter, J. B.; Penfold, J. *Colloid Polym. Sci.* **1983**, *261*, 1022. (b) Hayter, J. B.; Penfold, J. *Mol. Phys.* **1981**, *42*, 109. (c) Hansen, J.-P.; Hayter, J. B. *Mol. Phys.* **1982**, *46*, 109. (d) Hayter, J. B.; Penfold, J. *J. Chem. Soc., Faraday Trans. 1* **1981**, *77*, 1851.

(18) Mortensen, K. *J. Phys.: Condens. Matter* **1996**, *8*, A103.

(19) Israelachvili, J. N.; Marcelja, S.; Horn, R. G. *Q. Rev. Biophys.* **1980**, *13*, 121.

(20) Tanford, C. *J. Phys. Chem.* **1972**, *76*, 3020.

(21) (a) Frindi, M.; Michels, B.; Levy, H.; Zana, R. *Langmuir* **1994**, *10*, 1140. (b) Zana, R.; Benrraou, M.; Rueff, R. *Langmuir* **1991**, *7*, 1072.

(22) Blatt, F.; Ghiggino, K. P.; Sawyer, W. H. *J. Phys. Chem.* **1982**, *86*, 4461.

(23) (a) Rubingh, D. N. In *Solution Chemistry of Surfactants*; Mittal, K. L., Ed.; Plenum: New York, 1979; p 337. (b) Bucci, S.; Fagotti, C.; De Giorgio, V.; Piazza, R. *Langmuir* **1991**, *7*, 824. (c) Malliaris, A.; Binana-Limbele, W.; Zana, R. *J. Colloid Interface Sci.* **1986**, *110*, 114. (d) Velazquez, M. M.; Costa, S. M. B. *J. Chem. Soc., Faraday Trans.* **1990**, *86*, 4043. (e) Rathman, J. F.; Scamehorn, J. F. *J. Phys. Chem.* **1984**, *88*, 5807.